

Dynamical scattering of x-rays in vibrating deformed crystals

F. N. Chukhovskii, V. L. Nosik, and E. M. Iolin

A. V. Shubnikov Crystallography Institute, Russian Academy of Sciences

(Submitted 15 January 1993)

Zh. Eksp. Teor. Fiz. **104**, 2452–2472 (July 1993)

We develop a consistent theory for the dynamic scattering of x rays in a vibrating deformed crystal for the case when the ultrasound wavelength λ_s is much smaller than the extinction length Λ . We construct a picture of the propagation of the wave field in the crystal which is based upon a representation of Bloch waves responding to the motion of the x-ray quantum with the emission and also both with and without the absorption of phonons. We pay special attention to evaluating the integral diffraction coefficient (IDC), I_h^{int} , which is a function of two parameters: the modulus of the amplitude $|\mathbf{w}|$ of the ultrasound wave and the gradient of the deformation B of the crystal lattice. We show that under well defined circumstances I_h^{int} depends anomalously (nonmonotonically) on the amplitude $|\mathbf{w}|$ of the ultrasound wave (it goes through a minimum) for fixed values of B . The theory developed here explains quantitatively recently performed experimental measurements of the anomalous behavior of I_h^{int} .

1. INTRODUCTION

It was shown in the first papers on the effect of acoustic vibrations on the dynamic scattering of x rays (see, for instance, the review in Ref. 1) that it is possible in principle to measure the amplitude w of the ultrasound wave and also to determine the structure of the normal modes in piezoelectric transducers and resonators.

Later on the method of ultrasound action on the Bragg diffraction of x rays, and also of neutrons, was used to study a broad range of acousto-electronic, magneto-acoustic, and acousto-magnetic effects in perfect crystals.^{2,3}

The basic propositions of a classical theory of the dynamic diffraction in perfect crystals, in which an ultrasound wave is excited with a sinusoidal periodic atomic displacement field, were formulated in Refs. 4 to 6. A characteristic parameter of the diffraction problem is then the ratio of the ultrasound wavelength λ_s to the extinction length Λ of the x rays.

We restrict ourselves in what follows to the $\lambda_s \ll \Lambda$ case (high-frequency ultrasound) when positive gaps occur in the dispersion surface (DS; see Fig. 1), the magnitude of which corresponds to the renormalized value of the structure factor of the Bragg reflections.^{5,6} Physically the new gaps in the multi-sheeted DS correspond to diffraction reflections with the absorption or emission of n phonons (n th order satellites, $n=0, \pm 1, \pm 2, \dots$).

A convenient formalism for the description of the Bragg diffraction in vibrating crystals was proposed in Refs. 4 to 6 (see also Refs. 7 and 8) which was based upon expanding the amplitudes of the passing and the diffracted waves in Fourier series in the wave vector of the high-frequency ultrasound wave. In the angular region of each satellite one then takes into account only the two corresponding components of this expansion. This makes it possible, in principle, to reduce the problem to the canonical form of the dynamic theory (two-wave approximation).

Recently an exact solution of the diffraction problem in

a vibrating crystal was obtained in Ref. 9 when up to two components were taken into account in the expansions for the passing and the diffracted waves (four-wave approximation). It was shown that in the case of high-frequency ultrasound the corrections to the “two-wave” amplitude of the passing (diffracted) wave and the shape of the DS were, as to order of magnitude, equal to $(\Lambda/\lambda_s)^{-1}$ and $(\Lambda/\lambda_s)^{-2}$, respectively.

In the case of a vibrating crystal with a high-frequency ultrasound wave the integral diffraction coefficient (IDC) I_h^{int} can be written as a sum of scattering intensities $I_{h,n}^{\text{int}}$ for all satellites and the main reflection. Theoretically and experimentally it is known that the IDC for diffraction by a vibrating perfect crystal goes beyond the kinematic limit when the amplitude $h\mathbf{w}$ (\mathbf{h} is the diffraction vector) of the high-frequency ultrasound wave increases.^{4,6} Physically this is connected with the fact that with increasing $h\mathbf{w}$ the structure factor of each satellite diminishes and the diffraction scattering in the angular region of each satellite takes on a kinematic character. In the case of a nonabsorbing diffracting crystal the IDC therefore increases on the whole from its dynamic value for $h\mathbf{w}=0$ to the kinematic one for $h\mathbf{w} \rightarrow \infty$ which, in principle, agrees with the general statement⁸ that I_h^{int} increases when the deformation of the crystal lattice increases.

However, the situation becomes more complicated in the case of ultrasound excited in a deformed (for instance, a bent) crystal. It has been shown experimentally^{10,11} that I_h^{int} depends anomalously (nonmonotonically) on the amplitude of the ultrasound wave with a minimum at a voltage $V \approx 4$ V on the piezoelectric transducer.

Interbranch scattering when the excitation point passes through angular regions of satellites which are close to the main reflection was indicated in Ref. 10 as a possible cause for the anomalous dependence of the IDC I_h^{int} on $h\mathbf{w}$ for fixed values of B . The considerations in Ref. 10 are based upon a quasiclassical description of the dynamics of the

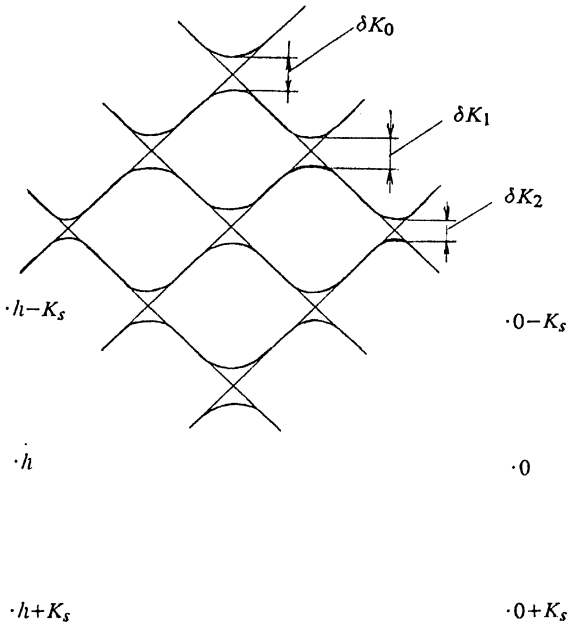


FIG. 1. Six-sheeted DS. We show the distances between the sheets of the DS for different satellites, $\delta K_n = 2\pi |J_n(\mathbf{h}\mathbf{w})|/\Lambda$, $n=0,1,2$.

excitation points and, hence, the results of Ref. 10 are applicable only when $B \ll 1$.

In the present paper we construct a consistent dynamic theory of the diffraction of a spherical wave by a deformed crystal in which high-frequency ultrasound is excited. Our exposition is based on a Green function formalism (point-source functions). We show that the parameter in our problem is the ratio of the angular distance $\Delta\theta_d$, traversed by the excitation point owing to the deformation, to the distance between satellites,

$$\Delta\theta_s = K_s/2k_0 \sin \theta,$$

where θ is the Bragg angle, K_s the wave vector of the ultrasound wave, and k_0 the wave vector of the passing wave.

In the special case of diffraction by a crystal with a constant deformation gradient, the angular distance traversed by the excitation point is equal to

$$\Delta\theta_d = 2\pi T B / (\Lambda k_0 \sin \theta),$$

where $T = t\pi/\Lambda$, t is the thickness of the crystal,

$$4B = \left(\frac{\Delta}{\pi}\right)^2 \frac{\partial^2 \mathbf{h}\mathbf{u}_d}{\partial s_0 \partial s_h}$$

and \mathbf{u}_d is the displacement vector in the static deformation field.

For $2BT < \Delta K$, where $\Delta K = \Lambda k_0 \sin \theta \Delta\theta_s/\pi$, each excitation point passes through at most one turning point (a point where locally the Bragg condition is satisfied). Under that condition we can use for describing the diffraction near a separate n th satellite the well known expressions for the Green function in a crystal with a constant deformation gradient with a renormalized extinction length. The

total Green function is a superposition of the Green functions corresponding to the different satellites.

One can easily show that for $\Delta K < 2BT < 2\Delta K$ the excitation point passes successively through two turning points. For $2\Delta K < 2BT < 3\Delta K$ the excitation point passes through three turning points, and so on. When the excitation point passes through several turning points there occurs a redistribution of the excitation between the branches of the DS due to the inter- and intra-branch scattering of Bloch waves in the crystal.

These physical considerations enable us to develop for diffraction by vibrating deformed crystals a consistent dynamical theory which we present in what follows.

2. STATEMENT OF THE PROBLEM. BASIC EQUATIONS

For simplicity we restrict ourselves in what follows to considering symmetric diffraction scattering of an x ray with a Bragg angle θ . We introduce a non-orthogonal dimensionless system of coordinates s_0, s_h with axes directed along the wave vectors \mathbf{k}_0 of the passing and \mathbf{k}_h of the diffracted waves such that

$$\mathbf{r} = (s_0 \mathbf{e}_0 + s_h \mathbf{e}_h) / \gamma, \quad (1)$$

where \mathbf{e}_0 and \mathbf{e}_h are the unit vectors along the axes of the non-orthogonal coordinate system and $\gamma = \cos \theta$.

All distances are measured in what follows in units Λ/π where Λ is the extinction length:

$$\Lambda = \lambda \gamma / (\chi_{hr} \chi_{-hr} - \chi_{hi} \chi_{-hi})^{1/2} \mathcal{C},$$

λ is the wavelength, \mathcal{C} is a polarization factor, equal to unity or $\cos 2\theta$, respectively, for σ or π polarization of the incident radiation,

$$\chi_{hi} = \text{Im}(\chi_h), \quad \chi_{hr} = \text{Re}(\chi_h),$$

and χ_h is the Fourier component of the polarizability of the crystal.

The coordinates (s_0, s_h) in the non-orthogonal system are connected with the coordinates (x, z) in the Cartesian coordinate system through the relations

$$x = (s_0 - s_h) \text{tg } \theta, \quad z = s_0 + s_h, \quad (2)$$

the z -axis is here directed perpendicular to the entrance surface of the crystal and the x -axis antiparallel to the diffraction vector \mathbf{h} (see Fig. 2).

It is well known that the amplitudes of the passing and the diffracted waves of the x-ray field in the point \mathbf{r} in the crystal are determined by integral convolutions of the Green functions $G_0(\mathbf{r}, \mathbf{r}')$, $G_h(\mathbf{r}, \mathbf{r}')$ and the amplitudes $E_0(\mathbf{r}')$ of the wave incident upon the crystal along the entrance surface of the crystal, $z=0$:

$$E_h(\mathbf{r}) = \int_{s'_0 = -s'_h} ds'_0 G_h(\mathbf{r}, \mathbf{r}') E_0(\mathbf{r}'), \quad (3)$$

$$E_0(\mathbf{r}) = \int_{s'_0 = -s'_h} ds'_0 G_0(\mathbf{r}, \mathbf{r}') E_0(\mathbf{r}').$$

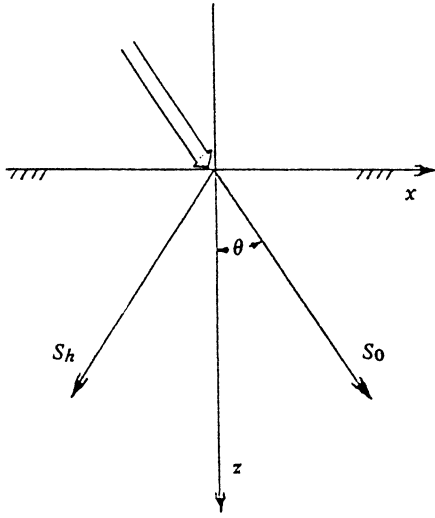


FIG. 2. Geometry of symmetric von Laue diffraction.

The Green functions in (3) (after exponential substitutions to account for the refraction of the x rays in the crystal) satisfy a system of inhomogeneous first-order partial differential equations:¹²

$$i \frac{\partial}{\partial s_0} G_0 + \sigma_{-h} \exp(i\mathbf{h}\mathbf{V}) G_h = i\delta(s_0 - s_0') \delta(s_h - s_h'), \quad (4)$$

$$i \frac{\partial}{\partial s_h} G_h + \sigma_h \exp(-i\mathbf{h}\mathbf{V}) G_0 = 0,$$

where the dynamic coefficients of the problem are equal to

$$\sigma_h = (1 + i\kappa)(\chi_{hr}/\chi_{-hr})^{1/2}, \quad \sigma_{-h} = (1 + i\kappa)(\chi_{-hr}/\chi_{hr})^{1/2},$$

and the normalized dynamic absorption coefficient κ is given by the expression

$$\kappa = (\chi_{hi}\chi_{-hr} + \chi_{-hi}\chi_{hr})/2(\chi_{hr}\chi_{-hr} - \chi_{hi}\chi_{-hi}).$$

The vector \mathbf{V} of the total displacement of the atoms from their equilibrium position can be written as a sum $\mathbf{u}_s + \mathbf{u}_d$ where \mathbf{u}_s is the displacement vector in the field of the standing transverse ultrasound wave:

$$\mathbf{h}\mathbf{u}_s = \mathbf{h}\mathbf{w} \cos(2\Delta Kz), \quad \mathbf{w} = \mathbf{u}_0 \cos(\omega t), \quad (5)$$

and \mathbf{u}_d the displacement which is quadratic in the field coordinates,

$$\mathbf{h}\mathbf{u}_d = 2(As_0^2 + 2Bs_0s_h + Cs_h^2). \quad (6)$$

Writing the Green functions G_g ($g=0, h$) in the form

$$G_0 = iQ_0 \exp(2iCs_h^2) \theta(s_0 - s_0') \theta(s_h - s_h') \exp\{-i\mathbf{h}\mathbf{u}(\mathbf{r}')\}, \quad (7)$$

$$G_h = iQ_h \exp(-2iAs_0^2) \theta(s_0 - s_0') \theta(s_h - s_h') \exp\{-i\mathbf{h}\mathbf{u}(\mathbf{r}')\},$$

and substituting them into (4) we find that the functions Q_g satisfy a system of homogeneous equations

$$i \frac{\partial}{\partial s_0} Q_0 + \sigma_{-h} Q_h \exp(i\mathbf{h}\mathbf{u}) = 0, \quad (8)$$

$$i \frac{\partial}{\partial s_h} Q_h + \sigma_h Q_0 \exp(-i\mathbf{h}\mathbf{u}) = 0,$$

where $\mathbf{h}\mathbf{u} = \mathbf{h} \cdot \mathbf{u}_s + 4Bs_0s_h$.

Using (4) it follows also from the definition (7) that the function Q_h on the characteristic lines $s_{h,0} = s'_{h,0}$ satisfies the following boundary conditions:

$$Q_h(s'_0, s_h; s'_0, s'_h) = 1, \quad (9)$$

$$Q_h(s_0, s'_h; s'_0, s'_h) = \exp\{i\mathbf{h}[\mathbf{u}(\mathbf{r}') - \mathbf{u}(s_0, s'_h)]\}. \quad (10)$$

For $\Delta K \gg 1$ (the case of a high-frequency ultrasound wave) we shall look for the solution of the set of Eqs. (8) in the form of an expansion

$$Q_g = \sum_{n=-\infty}^{\infty} Q_{g,n} \exp(2in\Delta Kz). \quad (11)$$

The set (8) then reduces to the following infinite set of partial differential equations

$$\left(-2n\Delta K + i \frac{\partial}{\partial s_h}\right) Q_{h,n} + \sigma_h \exp(-4Bis_0s_h) \times \sum_{m=-\infty}^{\infty} (-i)^{m-n} J_{m-n}(\mathbf{h}\mathbf{w}) Q_{0,m} = 0, \quad (12)$$

$$\left(-2m\Delta K + i \frac{\partial}{\partial s_0}\right) Q_{0,m} + \sigma_{-h} \exp(4Bis_0s_h) \times \sum_{n=-\infty}^{\infty} i^{n-m} J_{n-m}(\mathbf{h}\mathbf{w}) Q_{h,n} = 0,$$

where the J_m are m th order Bessel functions of a real argument.

Substituting (11) into the boundary conditions (9) and (10) and using the well known Gegenbauer expansion

$$\exp\{i\mathbf{h}\mathbf{w} \cos(2\Delta Kz)\} = \sum_{n=-\infty}^{\infty} J_n(\mathbf{h}\mathbf{w}) i^n \exp(2in\Delta Kz),$$

we find that the functions $Q_{h,n}$ describing the diffraction with the excitation of n phonons satisfy the following boundary conditions:

$$Q_{h,n}(s_0, s'_h; s'_0, s'_h) = J_n(\mathbf{h}\mathbf{w}) i^n \times \exp\{i\mathbf{h}\mathbf{u}_s(\mathbf{r}') - 4iBs'_h(s_0 - s'_0)\}, \quad (13)$$

$$Q_{h,n}(s'_0, s_h; s'_0, s'_h) = J_n(\mathbf{h}\mathbf{w}) i^n \times \exp\{i\mathbf{h}\mathbf{u}_s(\mathbf{r}') - 2in\Delta K(s_h - s'_h)\}. \quad (14)$$

One usually restricts oneself when solving the problem of diffraction of x rays by a crystal in which a high-frequency ultrasound wave is excited to the so-called two-wave approximation, taking only the terms $Q_{0,0}$ and $Q_{h,n}$ into account near the n th satellite. In the $2m$ -wave approximation one takes into account m terms when solving the set (8). The closed set of equations obtained as a result describes together with (13) and (14) completely the

problem of diffraction scattering of x rays in a vibrating crystal with a constant deformation gradient and, as we shall show in what follows, is a methodological base for an analysis of the propagation of x-ray waves in such crystals.

3. PROPAGATION OF THE WAVE FIELD IN A CRYSTAL

In the case considered (high-frequency ultrasound wave), when $\Delta K \gg 1$, the angular distance $\Delta\theta_s$ between the satellites is much larger than the width of the Bragg reflection of the main reflection. The processes of diffraction scattering of x rays corresponding to each of the satellites can then be considered independently of one another.^{2,4,7}

Near the satellite corresponding to the diffraction of x rays with absorption of n phonons, the set (8) reduces to two equations for the amplitudes $Q_{0,0}$ and $Q_{h,n}$ (two-wave approximation)

$$i \frac{\partial}{\partial s_h} Q_{h,n} = (-i)^n \exp(-4iBs_0s_h) J_n(\mathbf{hw}) \sigma_h Q_{0,0} + 2n\Delta K Q_{h,n}, \quad (15)$$

$$i \frac{\partial}{\partial s_0} Q_{0,0} = i^n \exp(4iBs_0s_h) J_n(\mathbf{hw}) \sigma_{-h} Q_{h,n}.$$

The set of Eqs. (15) is, apart from the renormalization of the coefficients, the same as the corresponding equations of the theory of diffraction of x rays in a crystal with a constant deformation gradient.¹² An exact solution of the set (15) can, if we use (13) and (14), be written in the form [cf. (2.9) of Ref. 12]

$$Q_{h,n} = i^n J_n(\mathbf{hw}) \exp\{i\mathbf{h}\mathbf{u}_s(\mathbf{r}') - 4iBs'_h\xi_0 - 2in\Delta K\xi_h\} {}_1F_1 \times (-\nu_n, 1, -4iB\xi_0\xi_h), \quad (16)$$

where we have introduced the variables

$$\xi_0 = s_0 - s'_0, \quad \xi_h = s_h - s'_h,$$

${}_1F_1$ is a confluent hypergeometric function and ν_n is a parameter determining the nature of the diffraction scattering of x rays and has the form

$$\nu_n = iJ_n^2(\mathbf{hw})\sigma^2/4B, \quad \sigma^2 = \sigma_h\sigma_{-h}. \quad (17)$$

Using (7) and (16) to change to the Fourier representation of the "partial" Green function (see Ref. 13)

$$G_{h,n}(\mathbf{r}, \mathbf{r}') = \frac{i^n}{2\pi} \sqrt{\nu_n} J_n(\mathbf{hw}) \exp\left\{-\frac{i\pi\nu_n}{2} - iB[\xi_h^2 + 2\xi_0(s_0 + s'_h) - \xi_0^2]\right\} \int_{-\infty}^{\infty} d\eta_0 P_{h,n}(\eta_0, \xi_0, \xi_h) \times \exp\left\{\frac{i\eta_0(\xi_h - \xi_0)}{2} + in\Delta K(x - x') \text{ctg } \theta\right\}, \quad (18)$$

we find that the plane-wave harmonics $P_{h,n}(\eta_0, \xi_0, \xi_h)$ have the following form:

$$P_{h,n}(\eta_0, \xi_0, \xi_h) = \exp[-in\Delta K(z - z')] \times \{D_{-\nu_n}(-iY_n(0)) D_{-\nu_n-1}(-Y_n) - D_{-\nu_n-1}(-Y_n(0)) D_{\nu_n}(-iY_n)\}, \quad (19)$$

where

$$Y_n(0) = \sqrt{i/B}(\eta_0 + n\Delta K), \quad Y_n = \sqrt{i/B}(\eta + n\Delta K).$$

In (19) the parameter η , which is equal to

$$\eta(z) = \eta_0 + 2Bz, \quad (20)$$

is a linear function of the z coordinate and determines the deflection of the reflecting planes as the Bloch wave penetrates into the crystal. The fact that the argument of the Weber functions D_{ν_n} and $D_{-\nu_n-1}$ vanishes in (19),

$$\eta(Z_n) + n\Delta K = 0 \quad (21)$$

corresponds physically to the Bloch wave passing through the turning point Z_n (the point where locally the Bragg condition is satisfied for the n th satellite).

As the wave penetrates into the crystal, when for the change in the parameter of the deflection of the reflecting planes the relation

$$\Delta\eta(z) = 2Bz > \Delta K$$

is satisfied, the Bloch wave may pass through one or several turning points while in the reciprocal space this process corresponds to the motion of the excitation point taking into account transitions from one branch of the multi-sheeted DS to another (intra- and inter-branch scattering of the Bloch wave).

Let now a Bloch wave propagate in the crystal with an initial deflection η_0 in the range

$$-2\Delta K \ll \eta_0 \ll -\Delta K. \quad (22)$$

From the boundary conditions on the entrance surface and condition (22) it follows that in our case only the branch of the DS with the asymptote perpendicular to the radius \mathbf{k}_0 (Fig. 3) is excited in practice.

It is clear from Fig. 3 that as the wave penetrates into the crystal the excitation point will pass successively through the turning points $Z_1, Z_0, Z_{-1}, \dots, Z_{-n}$ the positions of which are determined by the expression [see (21)]

$$Z_n = -(n\Delta K + \eta_0)/2B. \quad (23)$$

Near the first turning point Z_1 there is thus excited a satellite corresponding to the intersection of two straight lines perpendicular to the radii \mathbf{k}_0 and $\mathbf{k}_h + \mathbf{K}_s$ (Fig. 3) and to the components $P_{0,0}(Y_1)$ and $P_{h,1}(Y_1)$ of the quasipolar Bloch wave. In accordance with (19) these components have the following form:

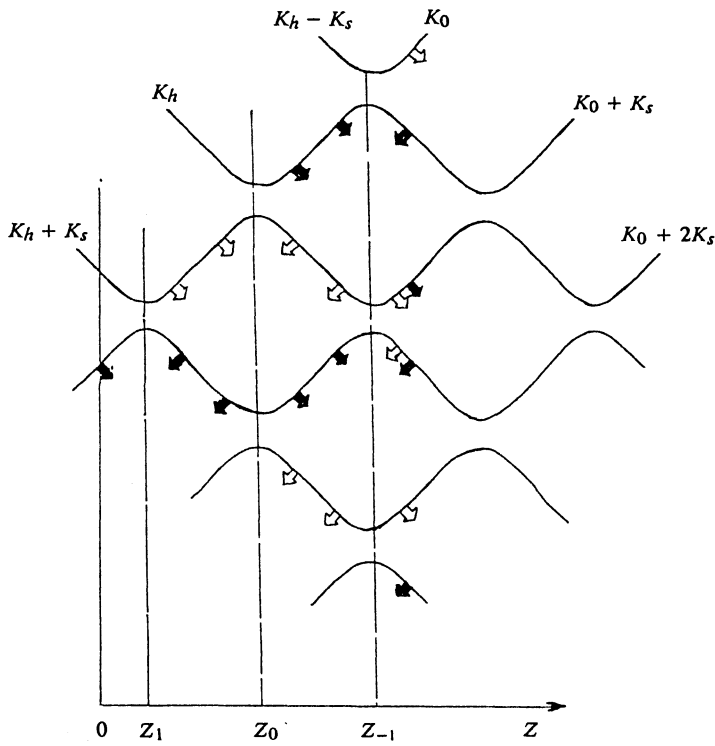


FIG. 3. Intra- and inter-branch scattering of a Bloch wave when it passes through three turning points.

$$\begin{aligned}
 P_{0,0}(Y_1) &= [M_1 D_{-\nu_1}(-Y_1) + N_1 D_{\nu_1-1}(-iY_1)] \\
 &\quad \times \exp(-i\Delta Kz), \\
 P_{h,1}(Y_1) &= [2\sqrt{iB/J_1(\hbar\omega)}] \exp(-i\Delta Kz) [\nu_1 M_1 D_{-1-\nu_1} \\
 &\quad \times (-Y_1) - iN_1 D_{\nu_1}(-iY_1)],
 \end{aligned} \tag{24}$$

Furthermore, near the turning point Z_0 , two satellites are excited corresponding to the pairwise intersection of two straight lines perpendicular, respectively, to the radii \mathbf{k}_0 , \mathbf{k}_h and $\mathbf{k}_0 + \mathbf{K}_s$, $\mathbf{k}_h + \mathbf{K}_s$ (Fig. 3). The x-ray waves corresponding to them are described by the following expressions:

$$\begin{aligned}
 P_{0,0}(Y_0) &= M_0^{(1)} D_{-\nu_0}(-Y_0) + N_0^{(1)} D_{\nu_0-1}(-iY_0), \\
 P_{h,0}(Y_0) &= [2\sqrt{iB/J_0(\hbar\omega)}] [\nu_0 M_0^{(1)} D_{-1-\nu_0}(-Y_0) \\
 &\quad - iN_0^{(1)} D_{\nu_0}(-iY_0)], \\
 P_{0,1}(Y_0) &= [M_0^{(2)} D_{-\nu_0}(-Y_0) + N_0^{(2)} D_{\nu_0-1}(-iY_0)] \\
 &\quad \times \exp(-2i\Delta Kz), \\
 P_{h,1}(Y_0) &= [2\sqrt{iB/J_0(\hbar\omega)}] \exp(-2i\Delta Kz) [\nu_0 M_0^{(2)} D_{-1-\nu_0} \\
 &\quad \times (-Y_0) - iN_0^{(2)} D_{\nu_0}(-iY_0)].
 \end{aligned} \tag{25}$$

The variables Y_1 and Y_0 in (24) to (26) are equal to

$$Y_1(z) = 2\sqrt{iB}(z - Z_1), \quad Y_0(z) = 2\sqrt{iB}(z - Z_0),$$

the coefficients M_1 and N_1 are determined from the boundary conditions at the entrance surface for $z=0$ and are equal to [see (19)]

$$M_1 = D_{-\nu_1-1}(-Y_1(0)), \quad N_1 = D_{-\nu_1}(-iY_1(0)), \tag{27}$$

while the coefficients $M_0^{(2)}$, $N_0^{(2)}$, $M_0^{(1)}$, and $N_0^{(1)}$ are determined from the solutions (24) to (26) for $z=z_*$, $Z_1 < z_* < Z_0$.

For simplicity we choose the point z_* where the solutions are joined to be

$$z_* = (Z_1 + Z_0)/2.$$

Assuming that the inequality $\sqrt{B} \ll \Delta K/2$ is satisfied and using the standard asymptotic form of the Weber functions we find by direct calculation

$$\begin{aligned}
 M_0^{(1)} &= [M_1 r_1 + N_1 t_1 \exp(i\varphi_1)] \\
 &\quad \times \exp[-iB(Z_1^2 - Z_0^2)] |Y_*|^{\nu_0 - \nu_1},
 \end{aligned} \tag{28}$$

$$\begin{aligned}
 N_0^{(2)} &= [N_1 r_1 + M_1 t_1 \exp(i\varphi_1)] \\
 &\quad \times \exp[iB(Z_1^2 - Z_0^2)] |Y_*|^{\nu_1 - \nu_0},
 \end{aligned} \tag{29}$$

$$M_0^{(2)}, N_0^{(1)} \propto 1/\Delta K \ll 1.$$

Here r_1 is the amplitude of the interbranch scattering and t_1 and φ_1 are the modulus and phase of the intrabranched scattering; they are given by the well known expressions

$$r_1 = \exp(-\pi|\nu_1|), \quad t_1^2 = (1 - r_1^2), \tag{30}$$

$$\varphi_1 = \text{Im}\{\ln[\Gamma(1 + i|\nu_1|)]\} + |\nu_1|(1 - \ln|\nu_1|) + \pi/4.$$

It follows from (28) and (29) that the coefficients $M_0^{(1)}$ and $N_0^{(2)}$ depend on the position of the joining point z_* ; this is a consequence of the simplified description of the

process of the propagation of the waves between the turning points Z_1 and Z_0 . A more correct analysis shows that one must replace the factor

$$\exp[-iB(Z_1^2 - Z_0^2) + i(|v_0| - |v_1|)\ln|Y_*|]$$

in (28) and (29) by the quantity

$$W_{1,0} = \exp\left[-i \int_{Z_1}^{Z_0} dz K_{1,0}(z) + v_0 \ln(2|v_0|^{1/2}) - v_1 \ln(2|v_1|^{1/2})\right], \quad (31)$$

where $K_{1,0}(z)$ is the quasimomentum of the Bloch wave calculated in the four-wave approximation (see Ref. 9),

$$K_{1,0}(z) = -\Delta K + \{[\Delta K - \sqrt{\eta^2 + J_0^2(\hbar\omega)}]^2 + J_1^2(\hbar\omega)\}^{1/2}. \quad (32)$$

Physically, the quantity $W_{1,0}$ is, apart from a constant coefficient, the advance in the phase of the Bloch x-ray wave when it propagates in the crystal between the turning points Z_1 and Z_0 .

One can easily show that the angular width δ_n of the n th satellite on the diffraction reflection curve is for $\Delta K > 2BT \gg |\chi_{h,n}|$ given by the expression

$$\delta_n = [(BT)^2 + |\chi_{h,n}|^2]^{1/2}. \quad (33)$$

Indeed, if we use the standard asymptotic form of the Weber functions ($|Y_n|, |Y_n(0)| \gg 1$), depending on the value of the parameter η_0 of the angular mismatch, the asymptotic expression for $P_{h,n}(\eta_0, \xi_0, \xi_n)$ in (19) takes the following forms

1) for $\eta_0 < -2BT$ and for $\eta_0 > 0$ we have

$$P_{h,n}(\eta_0, \xi_0, \xi_h) \approx (2\pi)^{-1} |v_n|^{1/2} \{ |Y_n(0)|^{v_n} |Y_n|^{-v_n-1} \times \exp[i(|Y_n(0)|^2 - |Y_n|^2)/4] + |Y_n|^{v_n} |Y_n(0)|^{-v_n-1} \times \exp[i(|Y_n|^2 - |Y_n(0)|^2)/4] \}, \quad (34)$$

2) for $0 > \eta_0 > -2BT$ we have

$$P_{h,n}(\eta_0, \xi_0, \xi_h) \approx (2\pi)^{-1} \{ |v_n|^{1/2} r_n |Y_n(0)|^{v_n} |Y_n|^{-v_n-1} \times \exp[i(|Y_n(0)|^2 - |Y_n|^2)/4] + r_n |v_n|^{1/2} |Y_n|^{v_n} |Y_n(0)|^{-v_n-1} \times \exp[i(|Y_n|^2 - |Y_n(0)|^2)/4] - t_n \exp(i\pi/4) |Y_n(0) Y_n|^{v_n} \times \exp[i(|Y_n(0)|^2 + |Y_n|^2)/4] - t_n \times \exp(i\pi/4) |v_n| |Y_n(0) Y_n|^{-v_n-1} \times \exp[i(|Y_n(0)|^2 + |Y_n|^2)/4] \}. \quad (35)$$

It is clear that in the angular regions $0 < \eta_0$ (to the right) and $\eta_0 < -2BT$ (to the left of the maximum of the n th satellite) the diffraction intensity $|P_{h,n}|^2$ decreases in proportion to $|Y_n(0)|^{-2}$ and $|Y_n|^{-2}$, respectively, whereas in the angular range $0 > \eta_0 > -2BT$ (the central part of the

peak) the intensity $|P_{h,n}|^2$ is independent of η_0 and is proportional to r_n^2 . We are thus led to the estimate (33) for the angular width of the satellite.

We now consider the case when for the incident wave on the entrance surface $z=0$ the inequality

$$|Y_1(0)| = (\eta_0 + \Delta K) / \sqrt{B} \gg 1$$

is satisfied. The coefficient N_1 occurring in (24) is then small as compared to M_1 :

$$|N_1|/|M_1| \approx |Y_1(0)|^{-1} \ll 1. \quad (36)$$

Moreover, one can simplify Eqs. (28) and (29) considerably under the conditions

$$|N_1|t_1/|M_1|r_1 \ll 1, \quad |N_1|r_1/|M_1|t_1 \ll 1,$$

which are simultaneously satisfied if we take (36) into account, provided

$$B_1 < B < B_2, \quad (37)$$

where the characteristic values of the constant deformation gradient are equal to

$$B_1 = \Delta K/2T, \quad B_2 = \Delta K/\sqrt{2\pi}. \quad (38)$$

For instance, for the experimentally possible values $\Delta K \approx 10$ and $T \approx 10$ we get $B_1 \approx 1/3$ and $B_2 \approx 4$.

If we use (36) and (37), Eqs. (28) and (29) take the form

$$M_0^{(1)} = M_1 r_1 W_{1,0}, \quad (39)$$

$$N_0^{(2)} = M_1 t_1 \exp(i\varphi_1) W_{1,0}^{-1}. \quad (40)$$

For large crystal thicknesses z such that

$$2Bz > 2\Delta K, \quad (41)$$

the x-ray Bloch wave traverses one more (a third) turning point Z_{-1} (see Fig. 3). Near the turning point Z_{-1} three satellites are excited corresponding on the DS to pairwise intersection of straight lines perpendicular to the radii \mathbf{k}_0 and $\mathbf{k}_h - \mathbf{K}_s$, $\mathbf{k}_0 + \mathbf{K}_s$ and \mathbf{k}_h , $\mathbf{k}_0 + 2\mathbf{K}_s$ and $\mathbf{k}_h + \mathbf{K}_s$.

Applying the same procedure we have used to derive Eqs. (39) and (40), and omitting the intermediate calculations we have found that near the turning point Z_{-1} the corresponding coefficients in the two-wave expansion (19) are equal to

$$M_{-1}^{(1)} = M_1 r_1 r_0 W_{1,0} W_{0,-1}, \quad (42)$$

$$N_{-1}^{(2)} = M_1 r_1 t_0 \exp(i\varphi_0) W_{1,0} W_{0,-1}^{-1}, \quad (43)$$

$$M_{-1}^{(2)} = M_1 t_1 \exp(i\varphi_1) r_0 W_{1,0}^{-1} W_{0,-1} \exp[2i\Delta K(Z_{-1} - Z_0)], \quad (44)$$

$$N_{-1}^{(3)} = M_1 t_0 \exp(i\varphi_0) r_1 W_{1,0}^{-1} W_{0,-1}^{-1} \exp[2i\Delta K(Z_{-1} - Z_0)]. \quad (45)$$

$$N_{-1}^{(1)}, M_{-1}^{(3)} \propto 1/\Delta K \ll 1.$$

One may thus say that in the general case a quasiplanar wave incident upon a crystal of thickness T such that

$$n\Delta K/2B < T < (n+1)\Delta K/2B,$$

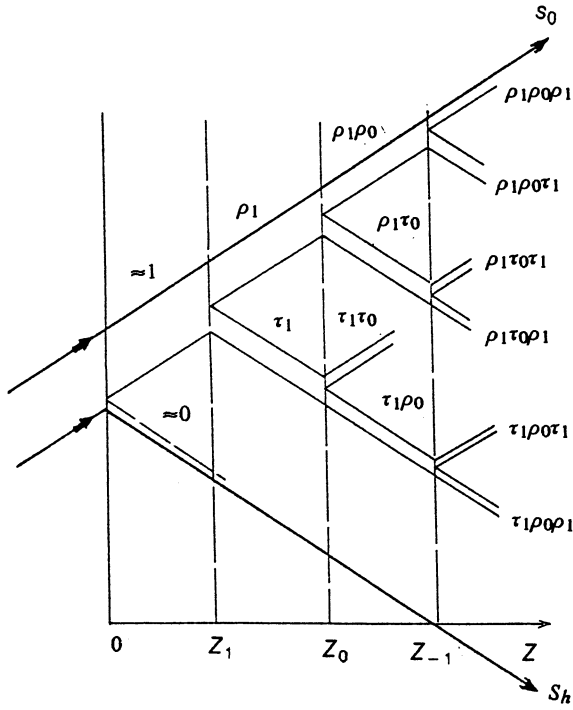


FIG. 4. Picture of the propagation and relative intensities of Bloch waves undergoing intra- and inter-branch scattering in a vibrating deformed crystal.

is, when leaving it, transformed into a superposition of $n+1$ Bloch waves; the probability that they are excited is the product of the probabilities of the intra- and inter-branch scattering as the result of successively passing through $n+1$ turning points.

As an illustration we show in Fig. 4 the trajectories of Bloch waves in a deformed vibrating crystal (the so-called "wave propagation tree"). On each branch of the "wave propagation tree" we show the probability for its excitation. On the entrance surface of the crystal only the passing wave is excited with a probability ≈ 1 . Propagating inside the crystal the wave successively passes through one, two, and three turning points corresponding to the diffraction of x rays with the emission and also both without and with the absorption of a single phonon.

4. THE ANOMALOUS BEHAVIOR OF THE INTEGRAL DIFFRACTION INTENSITY

It is well known that the IDC can be written as an integral of the square of the modulus of the Green function along the entrance surface of the crystal $z=0$:

$$I_h^{\text{int}} = \alpha \int_{-1}^1 |G_h(x, T; x - \xi T \operatorname{tg} \theta, 0)|^2 d\xi, \quad (46)$$

where T is the thickness of the crystal and $\alpha = \mathcal{C} |\chi_h| / 2 \sin \theta$.

Equation (46) together with the procedure for forming the "wave propagation tree" described in the preceding section enables us to calculate the IDC I_h^{int} as function of the two parameters \mathbf{hw} and B .

4.1. The $2BT < \Delta k$ case. One turning point

Substituting Eq. (16) for the Green function G_h into (46) one can write the IDC I_h^{int} in the form

$$I_h^{\text{int}} = \tilde{I}_h^{\text{int}} + \Delta I_h^{\text{int}}, \quad (47)$$

where \tilde{I}_h^{int} is the sum of the diffraction intensities corresponding to the different satellites:

$$\tilde{I}_h^{\text{int}} = \alpha \sum_{n=-\infty}^{\infty} J_n^2(\mathbf{hw}) \times \int_{-1}^1 |{}_1F_1(-\nu_n, 1, -iBT^2(1-\xi^2))|^2 d\xi, \quad (48)$$

and ΔI_h^{int} is the term describing the interference of the wave fields corresponding to the different satellites:

$$\Delta I_h^{\text{int}} = \alpha \sum_{\substack{n, n' = -\infty \\ n' \neq n}}^{\infty} J_n(\mathbf{hw}) J_{n'}(\mathbf{hw}) i^{n-n'} \times \int_{-1}^1 d\xi {}_1F_1(-\nu_n, 1, -iBT^2(1-\xi^2)) \times {}_1F_1^*(-\nu_{n'}, 1, -iBT^2(1-\xi^2)) \times \exp[i(n-n')\Delta KT(1+\xi)/2]. \quad (49)$$

It is clear from (49) that ΔI_h^{int} contains a fast oscillating factor $\exp[i(n-n')\Delta KT\xi/2]$ in the integration range $-1 \leq \xi \leq 1$. As a result, ΔI_h^{int} , in contrast to \tilde{I}_h^{int} contains a small parameter of order $(\Delta KT)^{-1} \ll 1$. Apart from terms proportional to $(\Delta KT)^{-1} \ll 1$ the IDC I_h^{int} is thus the sum of the diffraction intensities, $\tilde{I}_{h,n}^{\text{int}}$, corresponding to the different satellites.

For simplicity we consider the case of a nonabsorbing crystal. Using the quasiclassical asymptotic formulas for the Green function $G_{h,n}$ we find the following expression for the "partial" diffraction intensity $\tilde{I}_{h,n}^{\text{int}}$:

$$\tilde{I}_{h,n}^{\text{int}} = \alpha r_n^2 \int_{-1}^1 \frac{d\xi [J_n^2(\mathbf{hw}) + 2D^2(1-\xi^2)]}{(1-\xi^2)^{1/2} [J_n^2(\mathbf{hw}) + D^2(1-\xi^2)]^{1/2}}, \quad (50)$$

where $D = BT$.

Physically the meaning of Eq. (50) consists in that each n th satellite corresponds to renormalized values of the extinction length, $\Lambda_n = \Lambda / |J_n(\mathbf{hw})|$, the crystal thickness, $T_n = T |J_n(\mathbf{hw})|$, and the deformation gradient, $B_n = B |J_n(\mathbf{hw})|^2$.

In the $B_n T_n \ll 1$ limit Eq. (50) goes over into the corresponding expression $I_{h,n}^{\text{dyn}}$ for a perfect vibrating crystal (dynamic limit)

$$I_{h,n}^{\text{dyn}} = \pi \alpha |J_n(\mathbf{hw})|. \quad (51)$$

In the opposite limiting case, $B_n T_n \gg 1$, we get from (50)

$$\tilde{I}_{h,n}^{\text{int}} \approx 4 D \alpha r_n^2 \quad (52)$$

If, moreover, the intra-branch scattering coefficient is small, $r_n^2 \ll 1$, Eq. (52) goes over into the kinematic limit

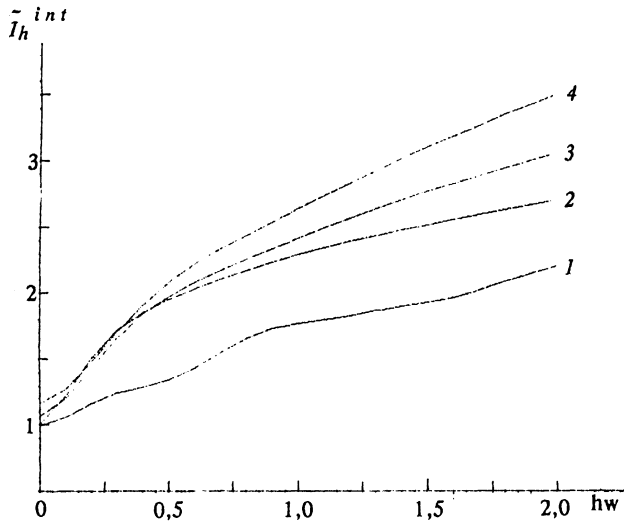


FIG. 5. \tilde{I}_h^{int} as function of the ultrasound wave amplitude hw for $z=12.8$, $B=0$ (curve 1), 0.01 (2), 0.02 (3), and 0.03 (4).

$$I_{h,n}^{kin} = 2\pi T \alpha J_n^2(hw). \quad (53)$$

In the general case we calculated the “partial” IDC $\tilde{I}_{h,n}^{int}$ by using Eq. (50) and the Gauss–Chebyshev numerical integration method.¹² Moreover, the results of the calculations using Eq. (50) which are given below were averaged over an oscillatory period of the standing ultrasound wave.

We show in Fig. 5 the IDC \tilde{I}_h^{int} as function of the amplitude of the ultrasound wave for $B=0, 0.01, 0.02$, and 0.03 (curves 1 to 4, respectively) for a crystal of thickness $z=12.8$, evaluated using Eq. (50) taking the $n=-5$ to 5 satellites into account. Notwithstanding the fact that the diffraction intensity $I_{h,n}^{int}$ for each satellite varies strongly as a function of the ultrasound wave amplitude, the total IDC \tilde{I}_h^{int} increases monotonically with increasing ultrasound wave amplitude, tending to the kinematic limit.

Before we turn to the case under consideration we make the following important remark which elucidates the physical meaning of Eq. (52).

It is clear from (52) that $\tilde{I}_{h,n}^{int}$ is the product of the deformation parameter, equal to the change in the angular deflection of the reflecting planes, $\delta\eta=2BT$ ($B>0$), over the total crystal thickness, and the probability $\tau_n=i_n^2$ for the intra-branch scattering of the quasi-planar Bloch wave. This means that the main contribution to the diffraction scattering, corresponding to the n th satellite, comes from the excitation points which during the motion change along the branch of the DS with an asymptote perpendicular to \mathbf{k}_0 to the corresponding part of the DS with an asymptote perpendicular to $\mathbf{h}+n\mathbf{K}_s$.

4.2. The $2\Delta K < 2BT < 3\Delta K$ case. Three turning points

Using Eqs. (39) and (40) we can derive expressions similar to (52) for the $\Delta K < 2BT < 2\Delta K$ case when the Bloch wave passes through two turning points. However, a

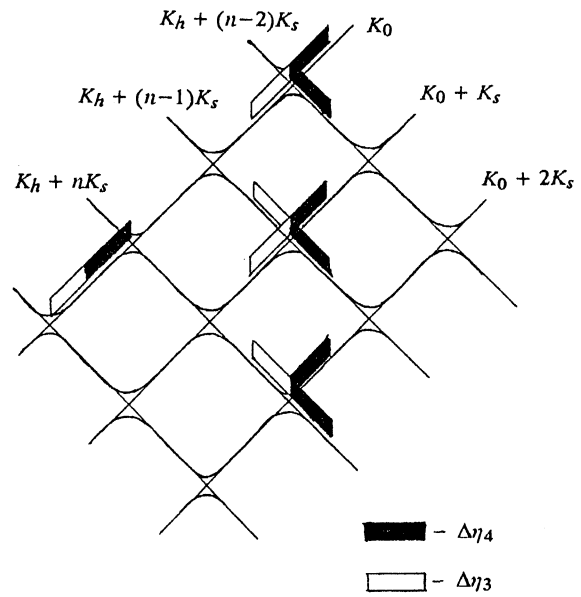


FIG. 6. Propagation of Bloch waves along the DS. We show the excitation points passing through three turning points in black and those passing through two turning points in white.

further consideration shows that the main interest will be in the case when the Bloch wave passes through at least three turning points.

In the case when the Bloch wave passes through three turning points, $2\Delta K < 2BT < 3\Delta K$ (see Fig. 6), using (42) to (45), we have instead of Eq. (52) for the “partial” IDC $\tilde{I}_{h,n}^{int}$

$$\tilde{I}_{h,n}^{int} = 2\alpha [\Delta\eta_4(\rho_n\rho_{n+1}\tau_{n+2} + \tau_n\tau_{n+1}\tau_{n+2} + \rho_n\tau_{n+1}\rho_{n+2} + \tau_n\rho_{n+1}\rho_{n+2}) + \Delta\eta_3(\rho_{n+1}\tau_n + \tau_{n+1}\rho_n)], \quad (54)$$

where $\Delta\eta_4 = 2BT - 2\Delta K$, $\Delta\eta_3 = 3\Delta K - 2BT$.

Summing the scattering intensities over all angular regions between the satellites we find a general expression for \tilde{I}_h^{int} :

$$\tilde{I}_h^{int} = 2\alpha \sum_{n=-\infty}^{\infty} [\Delta\eta_4(\rho_n\rho_{n+1}\tau_{n+2} + \tau_n\tau_{n+1}\tau_{n+2} + \rho_n\tau_{n+1}\rho_{n+2}) + \Delta\eta_4\tau_n\rho_{n+1}\rho_{n+2} + \Delta\eta_3(\rho_{n+1}\tau_n + \tau_{n+1}\rho_n)]. \quad (55)$$

We note that for $hw=0$ Eq. (55) changes into the corresponding expression for the IDC of a crystal with a constant deformation gradient, and in the limit of large deformations, when $|hw| \gg 1$ or $|B| \gg 1$ (but $2BT < 3\Delta K$) the IDC is the same as the kinematic value.

Generalizing what has been said above to the case of the successive passage of a Bloch wave through m turning points we can write the expression for the IDC \tilde{I}_h^{int} in the form

$$\tilde{I}_h^{int} = 2\alpha \sum_{m=-\infty}^{\infty} \left\{ \Delta\eta_m \sum_{j=1,3,5,\dots} L_{jm} + \Delta\eta_{m+1} \sum_{j=1,3,5,\dots} Q_{jm} \right\}. \quad (56)$$

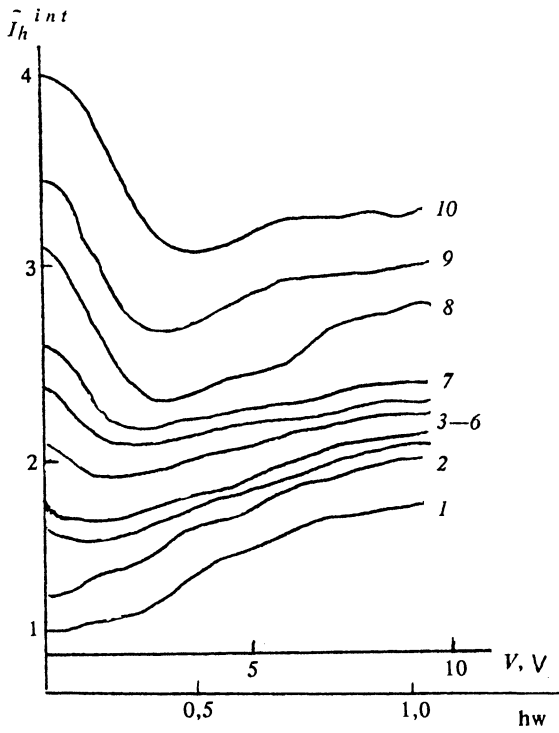


FIG. 7. Experimental curves of \tilde{I}_h^{int} as function of the ultrasound wave amplitude hw ; $T=360 \mu\text{m}$, $\Lambda=88.8 \mu\text{m}$, (660) reflection, for Si, and Mo K_α . The values of the characteristic parameters of the curves are given in the Table.

Here we have

$$\Delta\eta_m = 2BT - (m-1)\Delta K, \quad \Delta\eta_{m+1} = m\Delta K - 2BT,$$

and we have introduced the coefficients

$$L_{jm} = \sum_P f_n f_{n+1} f_{n+2} \dots f_{n+m-1}, \quad (57)$$

$$Q_{jm} = \sum_P f_n f_{n+1} f_{n+2} \dots f_{n+m-2},$$

where the summation over odd j is up to the fixed m . To evaluate L_{jm} and Q_{jm} one chooses for the terms f in the product all possible permutations from the series in which j of the elements are τ and $m-j$ of the elements are ρ . Each term in (57) is then physically the probability for the

creation of a Bloch wave undergoing j times intra- and $m-j$ times inter-branch scattering. For instance, the coefficient L_{14} corresponds to the sum of four terms:

$$L_{14} = \tau_n \rho_{n+1} \rho_{n+2} \rho_{n+3} + \rho_n \tau_{n+1} \rho_{n+2} \rho_{n+3} \\ + \rho_n \rho_{n+1} \tau_{n+2} \rho_{n+3} + \rho_n \rho_{n+1} \rho_{n+2} \tau_{n+3}.$$

5. COMPARISON BETWEEN THEORY AND EXPERIMENT

For a comparison of the theory with experiments we use the results of the measurement of the dependence of the IDC \tilde{I}_h^{int} on the voltage V on a piezoelectric transducer which were carried out in the Physics Institute of the Latvian Academy of Sciences (see Fig. 7, and also Fig. 4 from Ref. 11). The diffraction was studied of Mo K_α x rays by a vibrating Si crystal [thickness $t=360 \mu\text{m}$, (660) reflection, extinction length $\Lambda=88.8 \mu\text{m}$, third harmonic of a standing ultrasound wave with $\lambda_s=2t/3 \approx 240 \mu\text{m}$]. It is clear that one observes in deformed crystals on the initial sections of the function $\tilde{I}_h^{int}(V)$ an appreciable diminution of the intensity which reaches a maximum value of the order of 30% (anomalous behavior of the IDC \tilde{I}_h^{int}).

For a quantitative comparison of the experimental data with the results of our calculations it is necessary, starting from the experimental curve giving the function \tilde{I}_h^{int} , to calibrate the voltage V on the piezoelectric transducer by the magnitude of the ultrasound wave amplitude (hw) and to determine the magnitude of the constant deformation gradient B . To do this we determine the magnitude of B by describing the experimental points $\tilde{I}_h^{int}(hw=0; B)$ using the relation

$$[\tilde{I}_h^{int}(0, B) - \tilde{I}_h^{int}(0, 0)] / \tilde{I}_h^{int}(0, 0) = 4BT/\pi + \dots \quad (58)$$

which follows from (52) ($\pi/2 > B > 1/2T$).

We give in the Table the values of the constant deformation gradient calculated using Eq. (58) for the curves of Fig. 7. In the last column we give the number N of turning points traversed by the excitation points:

$$N = [2BT/\Delta K],$$

where $[x]$ is the integral part of the number x .

We give in Fig. 8 the results of the corresponding calculations of the IDC \tilde{I}_h^{int} as function of hw using Eqs. (52), (55), and (56) ($n=-5, \dots, 5$) as applied to the experimen-

TABLE I.

Number of the curve	$\tilde{I}_h^{int}(0, B) / \tilde{I}_h^{int}(0, 0)$	Deformation gradient, B	Number of turning points, N
1	1	0	—
2	1,2	0,07	2
3	1,77	0,108	3
4	1,89	0,12	3
5	2,14	0,13	3
6	2,34	0,148	3
7	2,56	0,15	3
8	3,1	0,189	4
9	3,43	0,21	4
10	4,0	0,244	5

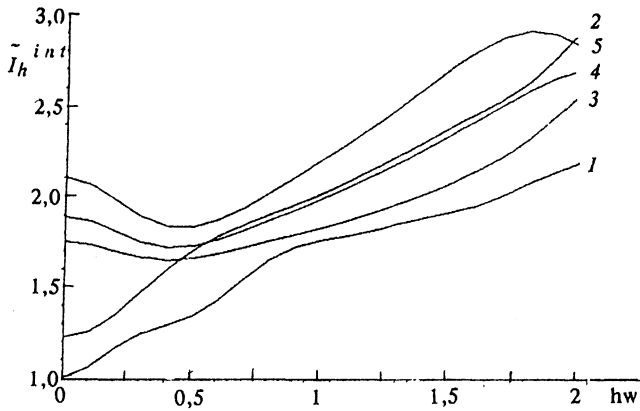


FIG. 8. Calculated functions $\tilde{I}_h^{int}(hw, V)$ for multiple passing of the wave through turning points. The values of the characteristic parameters of the curves are given in the Table.

tal data of Ref. 11: $\Delta K=1.1$, $T=12.8$. The calculated curves were averaged over an oscillation period of the ultrasound wave.

Furthermore, having in mind the construction of a calibration of the voltage V by the ultrasound wave amplitude hw we approximate the curve 1 ($B=0$) in Fig. 8 by a linear function using the least squares method. As a result the coefficient linking the ultrasound wave amplitude hw to the voltage V determined in this way is equal to 8.1 V.

The analysis shows (see the table) that in the case when the Bloch waves pass through one or two turning points the IDC \tilde{I}_h^{int} increases monotonically (see Fig. 8, curves 1 and 2). If the Bloch waves pass through three turning points there appears a local minimum on the curve showing the IDC \tilde{I}_h^{int} as function of hw which reaches a magnitude of 12%. Its position and magnitude then are, within an accuracy of $\pm 5\%$, the same as the corresponding experimental values (curves 3 to 5 in Figs. 7 and 8).

To calculate the IDC when the waves pass through four or more turning points one must use Eq. (56); the calculations show that the depth of the dip on the curve giving the IDC \tilde{I}_h^{int} as function of the ultrasound wave amplitude for fixed B initially increases with increasing parameter B , which determines the number of turning points which are passed through, but afterwards, starting with some values of B , the curve $\tilde{I}_h^{int}(hw)$ is smoothed out, going over into $\tilde{I}_{h,kin}^{int}$.

We give a qualitative explanation of this result, using the simple model proposed in Ref. 10. The results of numerical calculations show that the minimum of the curve of the IDC \tilde{I}_h^{int} function is formed for small values of the ultrasound wave amplitude ($hw \approx 0.4$) and small values of the deformation gradient, $B \ll \pi/2$, when the scattering of the Bloch waves in the angular region of the main reflection has an intra-branch character ($\rho_0 \rightarrow 0$) while the probability for the inter-branch scattering in the region of the n th satellite takes the form

$$\rho_n = \exp[-\pi(hw/2)^{2n}/2B], \quad n > 1.$$

Under these conditions the scattering in the region of the higher-order ($n \geq 2$) satellites has an essentially inter-branch character ($\tau_n \rightarrow 0$) so that we can neglect their effect when calculating the IDC:

$$\tilde{I}_h^{int} = 2\alpha[2\Delta K + 2(BT - \Delta K)(1 - 2\rho_1 + 2\rho_1^2)]. \quad (59)$$

One shows easily¹⁰ that in that approximation the position of the minimum hw_* on the curve of the function \tilde{I}_h^{int} is determined by the expression

$$hw_* = [8B \ln(2/\pi)]^{1/2}, \quad (60)$$

while the ratio of the IDC \tilde{I}_h^{int} at the minimum $\tilde{I}_h^{int}(hw_*, B)$ to the IDC \tilde{I}_h^{int} for a nonvibrating crystal $\tilde{I}_h^{int}(0, B)$ has the form

$$\tilde{I}_h^{int}(hw_*, B)/\tilde{I}_h^{int}(0, B) = 1/2 + \Delta K/2BT. \quad (61)$$

It follows from the experimental data (see Fig. 7 and the Table) that the $1/B$ dependence of the ratio $\tilde{I}_h^{int}(hw_*, B)/\tilde{I}_h^{int}(0, B)$ can be approximated by a linear function with an accuracy of 5%. The coefficient of this linear relation, calculated by the least squares method, turned out to be equal to 0.052 whereas the theory [see (61)] gives for it the value $\Delta K/2T = 0.043$.

For $B \gg \pi/2$ the scattering of the Bloch waves has an inter-branch character [$\tau_n \approx \pi(hw/2)^{2n}/2B$] in the angular region of all the satellites, and the general Eq. (55) can be written in the form of a series in powers of $\pi/2B$ with a first term which is the same as the kinematic limit for the IDC:

$$\tilde{I}_h^{int} = 4BT\alpha \left\{ \frac{\pi}{2B} - \left(\frac{\pi}{2B} \right)^2 \left[1 + 3(hw)^2 \frac{BT - \Delta K}{4BT} \right] + \dots \right\}.$$

In the region of intermediate B values we did not succeed in getting an explicit expression for the extremum of \tilde{I}_h^{int} as function of ρ_1 using Eq. (55).

In this approximation the maximum decrease in the IDC \tilde{I}_h^{int} in a vibrating deformed crystal thus reaches 50% for $\pi/2 \gg B \gg \Delta K/T$. The position of the minimum of the IDC, $h \cdot w_*$, for $B \ll \pi/2$ is described by Eq. (60), and when B increases further and there is a change to the kinematic diffraction regime the minimum disappears altogether. We note that the model considered agrees well with the results of numerical calculations and of experiments (see Figs. 7 and 8).

Summarizing, we can say that the phenomenon of an anomalous behavior of the IDC as function of the ultrasound wave amplitude in deformed crystals is connected with multiple intra- and inter-branch scattering of Bloch waves when they pass through three or more turning points.

In conclusion we note that qualitatively the phenomenon of an anomalous behavior of the IDC \tilde{I}_h^{int} as function of the ultrasound wave amplitude in deformed crystals was explained in Ref. 10 where it was assumed that the main contribution to the IDC comes from three turning points, including the main reflection. According to Ref. 10 the IDC \tilde{I}_h^{int} is determined by the expression [cf. (59)]

$$\tilde{I}_h^{int} \propto 1 - 2\rho_1 + 2\rho_1^2,$$

It is clear that this quantity reaches its minimum value $1/2$ for hw_* [see (60)] and that the magnitude of the minimum is, in general, independent of the deformation gradient B . However, the discussion given here shows that a quantitative agreement between the calculated and the experimental IDC is possible only in the framework of an exact theory, based on the Green function formalism, for the propagation of x-ray waves in vibrating deformed crystals.

- ¹W. Spencer, in *Physical Acoustics* (Ed. W. P. Mason) [Russ. transl.], Mir, Moscow, Vol. 5, p. 134.
²V. V. Kvardakov, V. A. Somenkov, and A. B. Tyugin, *Pis'ma Zh. Eksp. Teor. Fiz.* **48**, 396 (1988) [*JETP Lett.* **48**, 437 (1988)].
³V. V. Kvardakov and V. A. Somenkov, *Fiz. Tverd. Tela (Leningrad)* **31**, No 4, 235 (1989) [*Sov. Phys. Solid State* **31**, 680 (1989)].
⁴R. Kohler, W. Mohling, and H. Peibst, *Phys. Status Solidi* **B61**, 439 (1974).

- ⁵I. R. Éntin, *Zh. Eksp. Teor. Fiz.* **77**, 214 (1979) [*Sov. Phys. JETP* **50**, 110 (1979)].
⁶E. M. Iolin and I. R. Éntin, *Zh. Eksp. Teor. Fiz.* **85**, 1692 (1983) [*Sov. Phys. JETP* **58**, 985 (1983)].
⁷I. R. Entin, *Phys. Status Solidi* **B132**, 355 (1985).
⁸I. R. Entin, *Phys. Status Solidi* **A106**, 25 (1988).
⁹V. L. Nosik, *Kristallografiya* **36**, 1082 (1991) [*Sov. Phys. Crystallogr.* **36**, 610 (1991)].
¹⁰E. M. Iolin, É. A. Raïtman, B. V. Kuvaldin, and É. V. Zolotayabko, *Zh. Eksp. Teor. Fiz.* **94**, No 5, 218 (1988) [*Sov. Phys. JETP* **67**, 989 (1988)].
¹¹É. Zolotoyabko and V. Panov, *Acta Crystallogr.* **A48**, 225 (1992).
¹²F. N. Chukhovskii and P. V. Petrashen', *Acta Crystallogr.* **A33**, 311 (1977).
¹³F. Balibar, F. N. Chukovskii, and C. Malgrange, *Acta Crystallogr.* **A39**, 387 (1989).

Translated by D. ter Haar